

# Achievable Three-dimensional Quantum Ising Model Simulated with a Mixture of Ultracold Neutral Atoms

Ren Liao,<sup>1,\*</sup> Jingxin Sun,<sup>1</sup> Hui Li,<sup>1</sup> Shifeng Yang,<sup>1</sup> Pengju Zhao,<sup>2</sup> Xinyi Huang,<sup>1</sup>  
Wei Xiong,<sup>1</sup> Xiaoji Zhou,<sup>1</sup> Dingping Li,<sup>2</sup> Xiongjun Liu,<sup>2</sup> and Xuzong Chen<sup>1,†</sup>

<sup>1</sup>*School of Electronics Engineering and Computer Science, Peking University, Beijing 100871, China*

<sup>2</sup>*School of Physics, Peking University, Beijing 100871, China*

The low-energy effective model of a double-species Fermi-Hubbard (DSFH) model is analysed numerically with exact diagonalization method. When the lowest-energy subspace of the DSFH model is a Mott insulator of fermion pairs, the low-energy effective model is an exact antiferromagnetic Ising model with both transverse and longitudinal fields. Similarly, a ferromagnetic Ising model can be realized with a double-species Mott insulator of boson pairs. Such a realization of exact quantum Ising model allows us to investigate both the dynamics and thermodynamics of the Ising model in ultracold atom systems. And there is no limitation on the dimension of the lattice, which means the effective quantum Ising model in any achievable lattice configurations can all be simulated. These results may give some inspirations for experimental investigation of the exact solution of three-dimensional Ising model, classical and quantum critical phenomenon, quantum simulation of a spin liquid and other interesting topics related with the Ising model in ultracold atom systems.

Exact simulation of an ideal theoretical model with desired Hamiltonian, dimension and other properties is one of the major subjects of quantum simulation [1]. Such an exact realization of desired theoretical models acts as a bridge between theory and experiment, helping understanding many exotic behaviors of quantum particles and many important theoretical concepts. However, due to the limitations of various quantum simulation platforms [1], the achievable models are still quite few and usually not perfect. Realizing a specific model exactly still poses a big challenge to this area. Especially for those textbook models which shape our notions of many basic physics concepts, exact quantum simulation of these models could help clarify many uncertain parts and solidify the basis of these basic concepts.

One of the simplest textbook models is the quantum Ising model, which is frequently used as a toy model to understand quantum phase transition [2], quantum criticality [3, 4], dynamical quantum phase transition [5], quantum annealing [6], spin liquid [7] and spin ice [8] and many other important concepts. Though there are already many reported studies of simulating the quantum Ising model with trapped ions [9–13], Rydberg atoms [14–16], superconducting circuits [17–21], ultracold neutral atoms [22, 23] and quantum magnetic materials [24, 25], there are still limitations of these reported methods. Either a tunable and spatially independent spin-spin interaction cannot be realized, or the dimension of the lattice is limited, or the number of spins is too small, or the thermal equilibrium of the Ising model cannot be simulated. These defects restrict the potential application of these methods of simulating a quantum Ising model.

In this letter, we show that an ideal textbook model of the Ising model without all the above defects is possible to be realized with a mixture of ultracold neutral atoms in an optical lattice. Such an exact simulation of Ising model allows us to investigate both the dynamics

and thermodynamics of the Ising model. And there is no limit on the dimension of the lattice, which means  $n$ -dimensional ( $nD$ ,  $n = 1, 2, 3$ ) quantum Ising model in any achievable lattice configurations can all be simulated. These features enable us to conduct a more comprehensive research on the classical and quantum criticality of the Ising model experimentally, such as the measurement of various critical exponents ranging from the mean-field values ( $D \geq 4$ ) to the low-dimension values ( $D < 4$ ) taking into account of quantum-classical mapping [26]. Though in some magnetic materials, the quantum critical behaviors of some magnetic models has been revealed [24, 25, 27]. Quantum simulation of the Ising model with an optional dimension is still meaningful considering the superior controllability and various observation techniques of cold atom systems. Meanwhile, searching for the exact solution of the 3D Ising model has been a hot topic in mathematical physics for decades. Only recently are there some important progressive results for this problem [28–30]. And there are many discussions about the integrability (solubility) of the Ising model under an external field in a 2D lattice [31, 32]. Exact quantum simulation of a 2D or 3D Ising model may help validate these results and deepen our understanding of quantum integrable system. Moreover, the exact simulation of the antiferromagnetic Ising model can also be applied to the quantum simulation of a large-scale spin liquid in a lattice with strong geometrical frustration. Comparing with the spin liquid found in some magnetic materials by neutron scattering and magnetic excitation spectrum [33–36], cold atom systems could provide more determined evidence of the microscopic behaviors of a spin liquid. Using the quantum gas microscope technique [37], it is possible to study the exotic features of a spin liquid with a site-resolved resolution. With these considerations, it is promising to simulate an exact Ising model

with an optional dimension in an optical lattice.

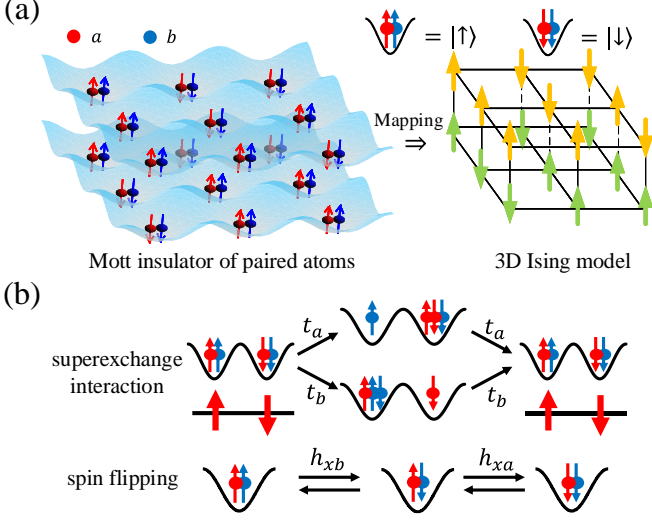


FIG. 1. The realization of the exact 3D Ising model with a Mott insulator of paired atoms. At each site,  $|n_{i\uparrow}^a = 1, n_{i\uparrow}^b = 1\rangle$  and  $|n_{i\downarrow}^a = 1, n_{i\downarrow}^b = 1\rangle$  can be mapped to spin up and down of a single spin, respectively. (b) The second-order superexchange interaction between two nearest-neighbor atom pairs is diagonal (no spin-exchange interaction) so that the effective spin-spin interaction is an Ising-like interaction. The spin flipping of an atom pair can be induced by the second-order flipping of each species of atoms in each lattice site.

*Theoretical Model.*— Considering a mixture of two-species of fermionic atoms populated in the lowest band of a deep lattice, the Hamiltonian can be described by a double-species Fermi-Hubbard (DSFH) model

$$\hat{H}^f = \hat{H}_a^f + \hat{H}_b^f + \hat{H}_{ab}, \quad (1)$$

$$\begin{aligned} \hat{H}_{s=a,b}^f = & -t_s \sum_{\sigma=\uparrow\downarrow} \sum_{\langle ij \rangle} (\hat{s}_{i\sigma}^\dagger \hat{s}_{j\sigma} + H.c.) + U_s \sum_i \hat{n}_{i\uparrow}^s \hat{n}_{i\downarrow}^s \\ & - \sum_i \frac{h_{zs}}{2} (\hat{n}_{i\uparrow}^s - \hat{n}_{i\downarrow}^s) - \sum_i h_{xs} (\hat{s}_{i\uparrow}^\dagger \hat{s}_{i\downarrow} + H.c.), \end{aligned}$$

$$\hat{H}_{ab} = \sum_{\sigma=\uparrow\downarrow} \sum_i (U_{ab}^+ \hat{n}_{i\sigma}^a + U_{ab}^- \hat{n}_{i\sigma}^a) \hat{n}_{i\sigma}^b. \quad (2)$$

Here  $\hat{s}_{i\sigma}^\dagger, \hat{s}_{i\sigma}$  ( $s = a, b$ ) are the fermionic creation and annihilation operators of the two species of atoms  $a$  and  $b$ .  $\hat{n}_{i\sigma}^s = \hat{s}_{i\sigma}^\dagger \hat{s}_{i\sigma}$  are the particle number operators.  $\uparrow$  ( $\downarrow$ ) represents spin up (down) and  $\bar{\sigma}$  is the inverse spin of  $\sigma$ . And  $t_s, h_{xs}$  and  $h_{zs}$  are the nearest-neighbor tunneling energy, the spin-flipping energy and the magnetic energy in an external field, respectively.  $\langle ij \rangle$  represents the nearest-neighbor lattice sites.  $U_{ab}^+, U_{ab}^-$  and  $U_s$  are the on-site interaction between different atom pairs in each lattice site. Defining  $U_{ab} = U_{ab}^+ - U_{ab}^-$ , we assume  $U_{ab} > 0$  and the magnitude of these parameters are assumed to satisfy  $t_s, h_{xs}, h_{zs} \ll U_s, U_{ab}$  so that the ground state of this model is a Mott insulator when each lattice site is

filled with only one  $a$  atom and one  $b$  atom. A positive  $U_{ab}$  guarantees that there are only two possible occupation states  $|\hat{n}_{i\uparrow}^a = 1, \hat{n}_{i\uparrow}^b = 1\rangle$  and  $|\hat{n}_{i\downarrow}^a = 1, \hat{n}_{i\downarrow}^b = 1\rangle$  in each lattice site for the lowest-energy subspace, which can be mapped to  $|\hat{S}_i^z = 1/2\rangle$  and  $|\hat{S}_i^z = -1/2\rangle$  of a single  $S = 1/2$  spin [Fig. 1(a)]. We denote  $|\hat{n}_{i\uparrow}^a = 1, \hat{n}_{i\uparrow}^b = 1\rangle$  and  $|\hat{n}_{i\downarrow}^a = 1, \hat{n}_{i\downarrow}^b = 1\rangle$  as  $|\uparrow\rangle_i$  and  $|\downarrow\rangle_i$  hereafter. Upon such a Mott insulator of fermion pairs, the second-order low-energy effective model of Eqn.(1) reads

$$\hat{H}_{\text{eff}}^f = J_z \sum_{\langle ij \rangle} \hat{S}_i^z \hat{S}_j^z - h_x \sum_i \hat{S}_i^x - h_z \sum_i \hat{S}_i^z \quad (3)$$

with

$$J_z = \sum_{s=a,b} \frac{4t_s^2}{U_{ab} + U_s}, h_x = \frac{4h_{xa}h_{xb}}{U_{ab}}, h_z = \sum_{s=a,b} h_{zs}.$$

Here  $\hat{S}_i^\alpha = \frac{1}{2}(|\uparrow\rangle_i \langle\downarrow|_i - |\downarrow\rangle_i \langle\uparrow|_i) \sigma^\alpha$  ( $\alpha = x, y, z$ ) and  $\sigma^\alpha$  are the Pauli matrices. Remembering the effective Heisenberg model originated from a Mott insulator of a single-species Fermi-Hubbard model [38], we could find the spin pairing between different species of atoms as a result of  $\hat{H}_{ab}$  is the key factor for the realization an exact Ising model [Fig.1(b)].

When we consider a mixture of two species of bosonic atoms, the Hamiltonian of a double-species Bose-Hubbard model can be written as

$$\hat{H}^b = \hat{H}_a^b + \hat{H}_b^b + \hat{H}_{ab}, \quad (4)$$

$$\begin{aligned} \hat{H}_{s=a,b}^b = & -t_s \sum_{\sigma=\uparrow\downarrow} \sum_{\langle ij \rangle} (\hat{s}_{i\sigma}^\dagger \hat{s}_{j\sigma} + H.c.) + U_s^{\uparrow\downarrow} \sum_i \hat{n}_{i\uparrow}^s \hat{n}_{i\downarrow}^s \\ & + \sum_i \sum_{\sigma=\uparrow\downarrow} \frac{U_s^{\sigma\sigma}}{2} \hat{n}_{i\sigma}^s (\hat{n}_{i\sigma}^s - 1) - \frac{h_{zs}}{2} (\hat{n}_{i\uparrow}^s - \hat{n}_{i\downarrow}^s) \\ & - \sum_i h_{xs} (\hat{s}_{i\uparrow}^\dagger \hat{s}_{i\downarrow} + H.c.). \end{aligned} \quad (5)$$

Here  $\hat{s}_{i\sigma}^\dagger, \hat{s}_{i\sigma}$  ( $s = a, b$ ) become bosonic operators and the definition of  $\hat{H}_{ab}$  is the same as Eqn.(2). The magnitude of these parameters still satisfy  $t_s, h_{xs}, h_{zs} \ll U_s^{\sigma\sigma'}, U_{ab}$ . With the same spin mapping in Fig. 1(a), the effective Hamiltonian becomes

$$\hat{H}_{\text{eff}}^b = J_z^b \sum_{\langle ij \rangle} \hat{S}_i^z \hat{S}_j^z - h_x^b \sum_i \hat{S}_i^x - h_z^b \sum_i \hat{S}_i^z \quad (6)$$

with

$$\begin{aligned} J_z^b = & \sum_{s=a,b} \left[ \frac{4t_s^2}{U_{ab} + U_s^{\uparrow\downarrow}} - \sum_{\sigma=\uparrow\downarrow} \frac{2t_s^2}{U_{ab} + U_s^{\sigma\sigma}} \right], h_x^b = h_x, \\ h_z^b = & \sum_{s=a,b} \left[ h_{zs} + \frac{2t_s^2}{U_{ab} + U_s^{\uparrow\downarrow}} - \frac{2t_s^2}{U_{ab} + U_s^{\uparrow\uparrow}} \right]. \end{aligned}$$

It can be seen that the ferromagnetic Ising model can

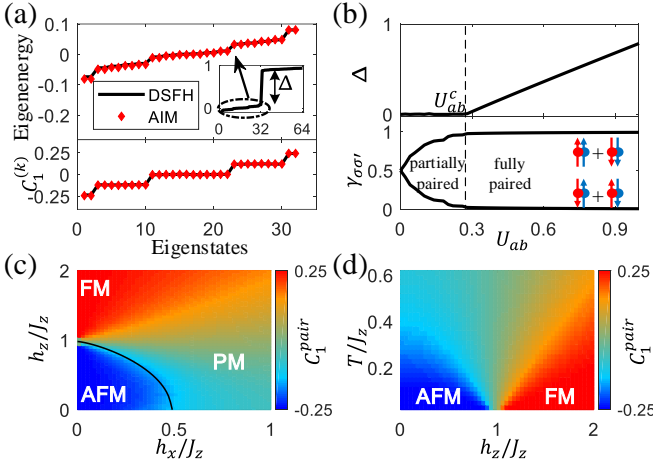


FIG. 2. Numerical validation of the effective antiferromagnetic Ising model. (a) The eigenenergy spectrum and nearest-neighbor spin correlations of the lowest  $2^L$  eigenstates of the 1D double-species Fermi-Hubbard (DSFH) model are in good agreement with those of the eigenstates of the effective 1D antiferromagnetic model (AIM). Here  $L = 5$  and  $k$  is the index of eigenstates. The inset is the eigenenergy spectrum of the lowest  $2^{L+1}$  eigenstates of the DSFH model. The parameters are set as  $J_a = J_b = 0.14$ ,  $U_a = U_b = U_{ab} = 1$ ,  $h_{xa} = h_{xb} = 0.05$ ,  $h_{za} = h_{zb} = 0$ . (b) The energy gap  $\Delta$  and the pairing ratio between different spins of a,b atoms  $\gamma_{\sigma\sigma'}$  with respect to  $U_{ab}$ . A large enough  $\Delta$  ( $\Delta \gg t_a, t_b$ ) and fully paired a,b atoms ( $\gamma_{\uparrow\uparrow} + \gamma_{\downarrow\downarrow} \rightarrow 1, \gamma_{\uparrow\downarrow} + \gamma_{\downarrow\uparrow} \rightarrow 0$ ) guarantee that the mapping to the Ising model is valid. (c) Simulation of the zero-temperature phase diagram of a 1D AIM chain with the DSFH model (with a lattice length  $L = 5$ ). The thick black line is the numerical result of the phase transition boundary of a  $L \rightarrow \infty$  AIM model given in Ref. [39]. (d) The quantum phase transition at the point  $h_z/J_z = 1, h_x/J_z = 0$  simulated with the DSFH model. Around this point, a V-shaped critical region can be seen in the  $h_z - T$  plane which is consistent with the effective Ising model.

also be exactly simulated if  $J_z^b < 0$ .

To make a quantitative validation of the effective antiferromagnetic Ising model [Eqn.(3)], we calculate the lowest-energy  $2^L$  eigenstates  $|\phi_k\rangle$  ( $k = 1, \dots, 2^L$ ) of the DSFH model in a one-dimensional lattice with a lattice size  $L = 5$ . The eigenenergy spectrum and the nearest-neighbor spin correlations  $C_1^{(k)} = \sum_{i=1}^{L-1} \langle \phi_k | \hat{S}_i^z \hat{S}_{i+1}^z | \phi_k \rangle / (L-1)$  of these eigenstates are in good agreement with those of the eigenstates of the effective Ising model [Fig. 2(a)]. And we could find a large energy gap  $\Delta = E_{2^L+1} - E_{2^L}$  above the lowest  $2^L$  eigenstates. Here  $E_k$  is just the eigenenergy of the  $k$ -th lowest eigenstate of the DSFH model.

To find when the a,b atoms begins to pair up with respect to  $U_{ab}$ , we calculate the ratio of the fermion pairs with different spins for the lowest  $2^L$  eigenstates  $\gamma_{\sigma\sigma'} = 2^{-L} \sum_{k=1}^{2^L} \sum_{i=1}^L \langle \phi_k | \hat{n}_{i\sigma}^a \hat{n}_{i\sigma'}^b | \phi_k \rangle / L$ . The results are shown in Fig. 2(b) and we could find that the a,b atoms become fully paired ( $\gamma_{\uparrow\uparrow} + \gamma_{\downarrow\downarrow} \rightarrow 1, \gamma_{\uparrow\downarrow} + \gamma_{\downarrow\uparrow} \rightarrow 0$ )

on the lowest  $2^L$  eigenstates with the increase of  $U_{ab}$  and an opening  $\Delta$ . And the onset of a nonzero  $\Delta$  determines a critical  $U_{ab}^c$  which is a parameter related with  $J_a, J_b$ . We usually set  $U_{ab} > (2 \sim 3)U_{ab}^c$  to ensure a better mapping to the effective Ising model [Eqn.(3)] and a large enough  $\Delta$  ( $\Delta \sim U_a, U_b$  and  $\Delta \gg J_z$ ).

*The phase diagram.*— Due to a large enough energy gap  $\Delta$  above the lowest  $2^L$  eigenstates, the partition function of the DSFH model  $Z = \text{tr}(e^{-\hat{H}/k_B T}) \approx \text{tr}(e^{-\hat{H}_{\text{eff}}/k_B T})$  when  $T \ll \Delta$ , which means the thermodynamics of the effective Ising model can be exactly simulated by the DSFH model. Here  $k_B$  is the Boltzmann constant and  $T$  is the temperature. As shown in Fig. 2(a), the zero-temperature phase diagram of an antiferromagnetic Ising chain is exactly simulated by the DSFH model. And the finite-temperature quantum phase transition at the point  $h_z/J_z = 1, h_x/J_z = 0$  in the  $h_z - T$  plane can also be obtained by the DSFH model [Fig. 2(b)]. Here we choose the point  $h_z/J_z = 1, h_x/J_z = 0$  instead of the typical point  $h_z/J_z = 0, h_x/J_z = 0.5$  to calculate the finite-temperature quantum phase transition is mainly due to a short lattice length in our numerical calculation. But this problem no long exists for experimental simulation of the quantum Ising model in a much larger lattice of hundreds of lattice sites.

Such an exact simulation of the thermodynamics of the quantum Ising model is a major advantage comparing with the former methods of simulating an Ising model. There is also no limit on the dimension of the lattice which may provide some convenience when considering experimental realization. More importantly, the effective mapping of the Ising model is based on the lowest-energy subspace of a Mott insulator so that this model is stable against various kinds of fluctuations. The only defect is that the magnetic interaction  $J_z$  induced by superexchange interaction is usually very weak, thus requiring a lower temperature to observe the magnetic orders induced by  $J_z$ . However, there are already experimental observations of weak magnetic orders induced by superexchange interaction under thermal equilibrium [40]. Therefore, the effective Ising model is achievable and observable with current experimental techniques.

*Simulation of a classical spin liquid.*— Searching for a quantum spin liquid in frustrated magnetic systems draws much of interest in recent years. The feature of a spin liquid is that there is no order in any spatial scale due to strong geometrical frustration even when  $T \rightarrow 0$ . Thus, it is a phase beyond the typical symmetry-breaking description and cannot be described by Ginzberg-Landau theory. Though there are many reported studies of finding a spin liquid in various kinds of quantum magnetic materials, there are still no deterministic evidence for realizing a clean spin liquid due to the limitations of the current observation methods. On the other hand, quantum simulation of frustrated magnetism provides another

route for experimental realization and observation of a spin liquid. And there are already some studies about the quantum simulation of frustrated magnetic models [10, 41]. In these experiments, the microscopic Hamiltonian can be easily controlled by experimental parameters so that more detailed information could be possibly obtained with such kind of quantum simulation methods. Nonetheless, quantum simulation of a large-scale spin liquid has still not been achieved. Here we show it is possible to obtain a large-scale classical spin liquid in an optical lattice with the above DSFH model.

The simplest case of a classical spin liquid is the antiferromagnetic Ising model in a triangular lattice. The spins cannot be aligned antiferromagnetically due to strong geometrical frustration. And one of the according results is a highly degenerate ground state subspace which has a degeneracy  $\Omega_0 \propto \alpha^{N_{spin}}$ . Here  $\alpha$  is a number dependent on the lattice configuration and  $N_{spin}$  is the number of spin. And the zero-point entropy per spin  $S_0 = \ln(\Omega_0)/N_{spin}$  is also nonzero in the thermodynamic limit  $N_{spin} \rightarrow \infty$  when  $T \rightarrow 0$ . As shown in Fig. 3(a), a 26-degree degenerate ground state subspace can be obtained for a six-site triangular lattice. From Fig. 3(b),  $S_0 = \ln(26)/6 \approx 0.543$  which is much larger than the theoretical value  $S_{0,theory} \approx 0.323$  [42, 43] of an infinitely large triangular lattice. By realizing a large enough triangular lattice, the long-known result of the zero-temperature entropy of  $0.323k_B$  per spin could be possibly validated with experiments. When a nonzero  $h_x$  breaks the ground-state degeneracy, the entropy per spin goes to zero quickly as  $T \rightarrow 0$ . Such a realization of a classical spin liquid can be implemented in a lattice with hundreds of lattice sites and can be used to experimental study of the universal properties of a spin liquid.

*The bosonic  $t - J_z$  model.* — If we change the repulsive interaction  $\hat{H}_{ab}$  with an attractive on-site interaction

$$\hat{H}'_{ab} = - \sum_{\sigma=\uparrow\downarrow} \sum_i (U_{ab}^+ \hat{n}_{i\sigma}^a + U_{ab}^- \hat{n}_{i\sigma}^b) \hat{n}_{i\sigma}^b \quad (7)$$

assuming  $U_{ab}^+ < U_{ab}^-$  at this time and redefining  $U_{ab} = U_{ab}^- - U_{ab}^+$ , the ground state of the DSFH model is still a Mott insulator of fermion pairs with the same spin pairing of a,b atoms as in Fig. 1(a). And the low-energy effective Ising model [Eqn. (3)] is still valid. The only difference is that such an attractive  $\hat{H}'_{ab}$  makes the a,b atom pairs stable against hole doping. With hole doping, the low-energy effective model would become a bosonic  $t - J_z$  model [Fig. 4(a)]

$$\begin{aligned} \hat{H}_{t-J_z} = & -t \sum_{\langle ij \rangle} \sum_{\sigma=\uparrow\downarrow} (\hat{B}_{i\sigma}^\dagger \hat{B}_{j\sigma} + H.c.) \\ & + J_z \sum_{\langle ij \rangle} (\hat{S}_i^z \hat{S}_j^z - \frac{\hat{n}_{iB} \hat{n}_{jB}}{4}) - J_{ph} \sum_{\langle ij \rangle} \hat{n}_{iB} \hat{n}_{jh} \end{aligned} \quad (8)$$

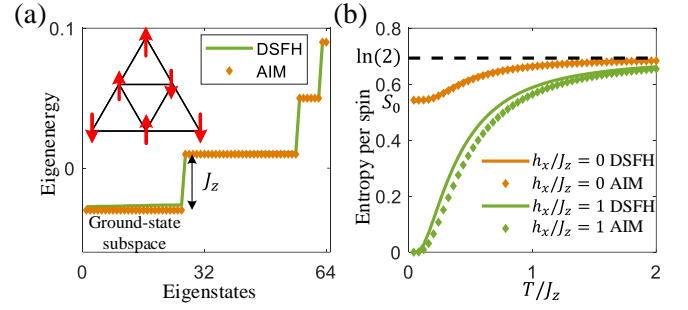


FIG. 3. Simulation of a classical spin liquid. (a) The energy spectrum of the antiferromagnetic Ising model (AIM) with  $h_x = 0, h_z = 0$  in a six-site triangular lattice simulated with the double-species Fermi-Hubbard model (DSFH). The inset shows the frustrated alignment of these spins of one of the ground states. A highly degenerate ground-state subspace indicates a classical spin liquid. (b) The entropy per spin of the frustrated antiferromagnetic Ising model with respect to the transverse field  $h_x$  and the temperature  $T$ . When  $h_x = 0$  and the ground-state degeneracy holds, a large zero-point entropy  $S_0 = \ln(26)/6$  can be seen even when  $T/J_z \rightarrow 0$ . When  $h_x > 0$  and the ground-state degeneracy breaks, the entropy per spin approaches 0 quickly as  $T/J_z \rightarrow 0$ . The parameters are set as  $J_a = J_b = 0.1, U_a = U_b = U_{ab} = 1, h_{za} = h_{zb} = 0$ .

with  $t = \frac{2t_a t_b}{U_{ab}}, J_{ph} = \frac{t_a^2 + t_b^2}{U_{ab}}$ . Here  $\hat{B}_{i\sigma} = \hat{a}_{i\sigma} \hat{b}_{i\sigma}$  is a bosonic annihilation operator and satisfies the hard-core boson limit  $\langle \hat{n}_{iB} \rangle \leq 1$  with  $\hat{n}_{iB} = \sum_{\sigma} \hat{B}_{i\sigma}^\dagger \hat{B}_{i\sigma}$ .  $\hat{n}_{ih} = 1 - \hat{n}_{iB}$  is the number of holes and  $J_{ph}$  is the interaction between nearest-neighbor particle-hole pairs. The bosonic  $t - J_z$  model is of interest as it reveals an unusual topological stripe phase under an antiferromagnetic background [44]. Comparing with the  $t - J$  model, the  $t - J_z$  model provides a simpler picture for the study of the phase diagram of a hole-doped antiferromagnet which is assumed to be related with the high-temperature superconductor of copper oxide. More experimentally achievable scenarios of such kind of models may help reveal the hidden mechanism of high-temperature superconductors.

To make a numerical calibration of the effective  $t - J_z$  model, we calculate the dynamical evolution of a five-site DSFH model from an initial state  $|\psi_0\rangle = |\uparrow, \downarrow, 0, \downarrow, \uparrow\rangle$  and use the number of holes at each site  $n_{ih}(\tau) = \langle \psi(\tau) | \hat{n}_{ih} | \psi(\tau) \rangle$  as an observable. Here  $\tau$  is the time and  $|\psi(\tau)\rangle$  is the wavefunction evolved from  $|\psi_0\rangle$  under the Hamiltonian of the DSFH model. The splitting, reflection on the border and recombination of the single hole in  $|\psi_0\rangle$  can be observed in the space-time map of  $n_{ih}(\tau)$  [Fig. 4(b)]. And the dynamical evolution of  $n_{ih}(\tau)$  is well consistent with that of the effective  $t - J_z$  model [Fig. 4(c)], validating the mapping of the  $t - J_z$  model.

*Conclusion and outlook.* — In summary, we have analyzed the low-energy effective model of the DSFH model. We show that the antiferromagnetic Ising model with achievable thermal equilibrium can be exactly simulated.



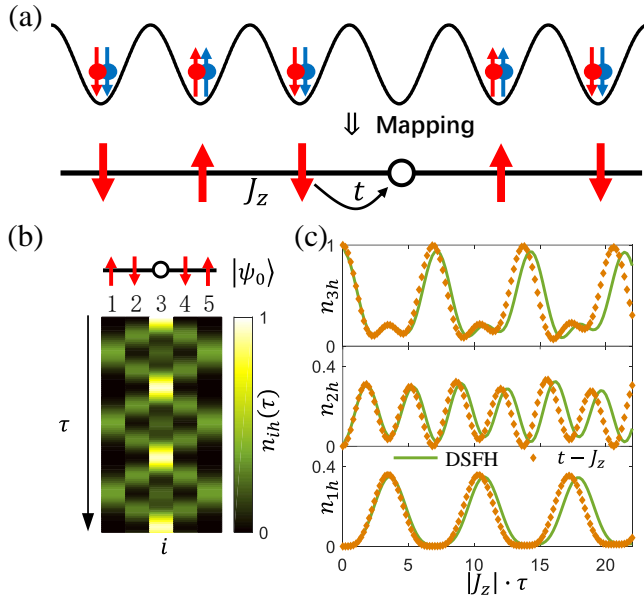


FIG. 4. Simulation of a bosonic  $t - J_z$  model. (a) The schematic of an effective  $t - J_z$  model. (b) The dynamical distribution of the number of holes  $n_{ih}$  evolved from an initial state  $|\psi_0\rangle$  simulated with the DSFH model. (c) The comparison of the  $n_{ih}(\tau)$  ( $i = 1, 2, 3$ ) simulated with the DSFH model and the  $n_{ih}(\tau)$  of the effective  $t - J_z$  model [Eqn. (8)]. The results show good consistency of these two models. The parameters are set as  $J_a = J_b = 0.1, U_a = U_b = 1, U_{ab} = 1, h_{za} = h_{zb} = 0, h_{xa} = h_{xb} = 0$ .

And there is no limit on the dimension of the lattice. Meanwhile, it is also possible to achieve a large-sacle classical spin liquid in the ultracold atom systems. Our results may provide some inspirations to experimental simulation of the quantum Ising model.

## ACKNOWLEDGEMENTS

This work is supported by the National Natural Science Foundation of China (Grants Nos. 11920101004, 11334001, 61727819, 61475007), and the National Key Research and Development Program of China (Grant No. 2021YFA1400900, 2021YFA0718300).

\* liaoren@pku.edu.cn

† xuzongchen@pku.edu.cn

- [1] I. M. Georgescu, S. Ashhab, and F. Nori, *Rev. Mod. Phys.* **86**, 153 (2014).
- [2] S. Sachdev, *Quantum Phase Transitions* (Cambridge University Press, New York, 2011).
- [3] P. Coleman and A. J. Schofield, *Nature* **433**, 226 (2005).
- [4] S. Sachdev and B. Keimer, *Physics Today* **64**, 29 (2011).
- [5] M. Heyl, A. Polkovnikov, and S. Kehrein, Vol. 110 (2013) p. 135704.

- [6] T. Kadowaki and H. Nishimori, *Phys. Rev. E* **58**, 5355 (1998).
- [7] L. Balents, *Nature* **464**, 199 (2010).
- [8] C. Castelnovo, R. Moessner, and S. L. Sondhi, *Nature* **451**, 42 (2008).
- [9] A. Friedenauer, H. Schmitz, J. T. Glueckert, D. Porras, and T. Schaetz, *Nature Physics* **4**, 757 (2008).
- [10] K. Kim, M.-S. Chang, S. Korenblit, R. Islam, E. E. Edwards, J. K. Freericks, G.-D. Lin, L.-M. Duan, and C. Monroe, *Nature* **465**, 590 (2010).
- [11] K. Kim, S. Korenblit, R. Islam, E. E. Edwards, M.-S. Chang, C. Noh, H. Carmichael, G.-D. Lin, L.-M. Duan, C. C. J. Wang, J. K. Freericks, and C. Monroe, *New Journal of Physics* **13**, 105003 (2011).
- [12] B. P. Lanyon, C. Hempel, D. Nigg, M. Müller, R. Gerritsma, F. Zähringer, P. Schindler, J. T. Barreiro, M. Rambach, G. Kirchmair, M. Hennrich, P. Zoller, R. Blatt, and C. F. Roos, *Science* **334**, 57 (2011).
- [13] J. W. Britton, B. C. Sawyer, A. C. Keith, C.-C. Joseph-Wang, J. K. Freericks, H. Uys, M. J. Biercuk, and J. J. Bollinger, *Nature* **484**, 489 (2012).
- [14] E. Guardado-Sanchez, P. T. Brown, D. Mitra, T. Devakul, D. A. Huse, P. Schauss, and W. S. Bakr, *Phys. Rev. X* **8**, 021069 (2018).
- [15] H. Labuhn, D. Barredo, S. Ravets, S. de Léséleuc, T. Macrì, T. Lahaye, and A. Browaeys, *Nature* **534**, 667 (2016).
- [16] P. Schauss, *Quantum Sci. Technol.* **3**, 023001 (2018).
- [17] Y. Salathe, M. Mondal, M. Oppliger, J. Heinsoo, P. Kurpiers, A. Potocnik, A. Mezzacapo, U. LasHeras, L. Lamata, E. Solano, S. Filipp, and A. Wallraff, *Phys. Rev. X* **5**, 021027 (2015).
- [18] M. Gong, X. Wen, G. Sun, D.-W. Zhang, D. Lan, Y. Zhou, Y. Fan, Y. Liu, X. Tan, H. Yu, Y. Yu, S.-L. Zhu, S. Han, and P. Wu, *Scientific Reports* **6**, 22667 (2016).
- [19] R. Barends, A. Shabani, L. Lamata, J. Kelly, A. Mezzacapo, U. L. Heras, R. Babbush, A. G. Fowler, B. Campbell, Y. Chen, Z. Chen, B. Chiaro, A. Dunsworth, E. Jeffrey, E. Lucero, A. Megrant, *et al.*, *Nature* **534**, 222 (2016).
- [20] R. Harris, Y. Sato, A. J. Berkley, M. Reis, F. Altomare, M. H. Amin, K. Boothby, P. Bunyk, C. Deng, C. Enderud, S. Huang, E. Hoskinson, M. W. Johnson, E. Ladizinsky, N. Ladizinsky, *et al.*, *Science* **361**, 162–165 (2018).
- [21] A. Cervera-Lierta, *Quantum* **2**, 114 (2018).
- [22] J. Simon, W. S. Bakr, R. Ma, M. E. Tai, P. M. Preiss, and M. Greiner, *Nature* **472**, 307 (2011).
- [23] R. Liao, F. Xiong, and X. Chen, *Phys. Rev. A* **103**, 043312 (2021).
- [24] R. Coldea, D. A. Tennant, E. M. Wheeler, E. Wawrzynska, D. Prabhakaran, M. Telling, K. Habicht, P. Smeibidl, and K. Kiefer, *Science* **327**, 177 (2010).
- [25] Y. Li, Q.-Y. Li, W. Li, T. Liu, D. J. Voneshen, P. K. Biswas, and D. Adroja, *npj Quantum Materials* **6**, 34 (2021).
- [26] M. Suzuki, *Progress of Theoretical Physics* **56**, 1454 (1976).
- [27] C. Ruegg, B. Normand, M. Matsumoto, A. Furrer, D. F. McMorrow, K. W. Kramer, H. U. Gudel, S. N. Gvasaliya, H. Mutka, and M. Boehm, *Phys. Rev. Lett.* **100**, 205701 (2008).
- [28] Z.-D. Zhang, *Philosophical Magazine* **87**, 34 (2007).

- [29] Z. Zhang, O. Suzuki, and N. H. March, [Advances in Applied Clifford Algebras](#) **29**, 12 (2019).
- [30] D. Zhang, [Symmetry](#) **13**, 10 (2021).
- [31] B. M. McCoy and J.-M. Maillard, [Progress of Theoretical Physics](#) **127**, 791 (2012).
- [32] Z. Zhang, [Physica E](#) **128**, 114632 (2021).
- [33] R. Coldea, D. A. Tennant, A. M. Tsvelik, and Z. Tylczynski, [Phys. Rev. Lett.](#) **86**, 1335 (2001).
- [34] X. Bai, J. Paddison, E. Kapit, S. Koohpayeh, J.-J. Wen, S. Dutton, A. Savici, A. Kolesnikov, G. Granroth, C. Broholm, J. Chalker, and M. Mourigal, [Phys. Rev. Lett.](#) **122**, 097201 (2019).
- [35] B. Gao, T. Chen, D. W. Tam, C.-L. Huang, K. Sasmal, D. T. Adroja, F. Ye, H. Cao, G. Sala, M. B. Stone, C. Baines, J. A. T. Verezhak, H. Hu, J.-H. Chung, X. Xu, *et al.*, [Nature Physics](#) **15**, 1052 (2019).
- [36] S. Janas, J. Lass, A.-E. Tũtueanu, M. L. Haubro, C. Nierdmayer, U. Stuhr, G. Xu, D. Prabhakaran, P. P. Deen, S. Holm-Dahlin, and K. Lefmann, [Phys. Rev. Lett.](#) **126**, 107203 (2021).
- [37] W. S. Bakr, J. I. Gillen, A. Peng, S. Folling, and M. Greiner, [Nature](#) **462**, 74 (2009).
- [38] E. Manousakis, [Rev. Mod. Phys.](#) **63**, 1 (1991).
- [39] A. A. Ovchinnikov, D. V. Dmitriev, and V. Y. Krivnov, [Phys. Rev. B](#) **68**, 214406 (2003).
- [40] A. Mazurenko, C. S. Chiu, G. Ji, M. F. Parsons, M. Kanász-Nagy, R. Schmidt, F. Grusdt, E. Demler, D. Greif, and M. Greiner, [Nature](#) **545**, 462 (2017).
- [41] J. Struck, C. Ölschläger, R. L. Targat, P. Soltan-Panahi, A. Eckardt, M. Lewenstein, P. Windpassinger, and K. Sengstock, [Science](#) **333**, 996 (2011).
- [42] G. H. Wannier, [Phys. Rev.](#) **79**, 357 (1950).
- [43] R. Houtappel, [Physica](#) **16**, 425 (1950).
- [44] J. Smakov, C. D. Batista, and G. Ortiz, [Phys. Rev. Lett.](#) **93**, 067201 (2004).